AFRL-RX-WP-TP-2012-0216

ON THE CORRELATION BETWEEN MORPHOLOGY OF α AND ITS CRYSTALLOGRAPHIC ORIENTATION RELATIONSHIP WITH TiB AND β IN BORON CONTAINING Ti-5Al-5Mo-5V-3Cr-0.5Fe ALLOY (PREPRINT)

P. Nandwana, S. Nag, and R. Banerjee
University of North Texas

D. Hill and H.L. Fraser,
Ohio State University

J. Tiley
Metals, Ceramics & Nondestructive Evaluation Division

JANUARY 2012

AIR FORCE RESEARCH LABORATORY
MATERIALS AND MANUFACTURING DIRECTORATE
WRIGHT-PATTERSON AIR FORCE BASE, OH 45433-7750
AIR FORCE MATERIEL COMMAND
UNITED STATES AIR FORCE

NOTICE AND SIGNATURE PAGE

Using Government drawings, specifications, or other data included in this document for any purpose other than Government procurement does not in any way obligate the U.S. Government. The fact that the Government formulated or supplied the drawings, specifications, or other data does not license the holder or any other person or corporation; or convey any rights or permission to manufacture, use, or sell any patented invention that may relate to them.

This report was cleared for public release by the USAF 88th Air Base Wing (88 ABW) Public Affairs Office and is available to the general public, including foreign nationals. Copies may be obtained from the Defense Technical Information Center (DTIC) (http://www.dtic.mil).

AFRL-RX-WP-TR-2012-0216 HAS BEEN REVIEWED AND IS APPROVED FOR PUBLICATION IN ACCORDANCE WITH ASSIGNED DISTRIBUTION STATEMENT.

//SIGNED//

JAY TILEY, Program Manager
Metals Branch
Metals, Ceramics & Nondestructive Evaluation Division

//SIGNED//

BRANCH CHIEF, Chief
Metals Branch
Metals, Ceramics & Nondestructive Evaluation Division

//SIGNED//

DIVISION CHIEF, Division Chief
Metals, Ceramics & Nondestructive Evaluation Division
Materials and Manufacturing Directorate

This report is published in the interest of scientific and technical information exchange, and its publication does not constitute the Government's approval or disapproval of its ideas or findings.

*Disseminated copies will show "//signature//" stamped or typed above the signature blocks.

REPORT DOCUMENTATION PAGE

Form Approved
OMB No. 0704-0188

1. REPORT DATE *(DD-MM-YY)*	2. REPORT TYPE	3. DATES COVERED *(From - To)*
January 2012	Technical Paper	1 November 2011 – 1 November 2011

4. TITLE AND SUBTITLE

ON THE CORRELATION BETWEEN MORPHOLOGY OF α AND ITS CRYSTALLOGRAPHIC ORIENTATION RELATIONSHIP WITH TiB AND β IN BORON CONTAINING Ti-5Al-5Mo-5V-3Cr-0.5Fe ALLOY (PREPRINT)

5a. CONTRACT NUMBER
FA8650-08-C-5226

5b. GRANT NUMBER

5c. PROGRAM ELEMENT NUMBER
62102F

6. AUTHOR(S)

P. Nandwana, S. Nag, D. Hill, J. Tiley, H.L. Fraser, and R. Banerjee

5d. PROJECT NUMBER
4347

5e. TASK NUMBER
00

5f. WORK UNIT NUMBER
LM114100

7. PERFORMING ORGANIZATION NAME(S) AND ADDRESS(ES)

University of North Texas
Corner of Ave. C Chestnut
Denten, TX 76203

Ohio State University
Metals, Ceramics & Nondestructive Evaluation Division

8. PERFORMING ORGANIZATION REPORT NUMBER
AFRL-RX-WP-TP-2012-0216

9. SPONSORING/MONITORING AGENCY NAME(S) AND ADDRESS(ES)

Air Force Research Laboratory
Materials and Manufacturing Directorate
Wright-Patterson Air Force Base, OH 45433-7750
Air Force Materiel Command
United States Air Force

10. SPONSORING/MONITORING AGENCY ACRONYM(S)
AFRL/RXLM

11. SPONSORING/MONITORING AGENCY REPORT NUMBER(S)
AFRL-RX-WP-TP-2012-0216

12. DISTRIBUTION/AVAILABILITY STATEMENT
Approved for public release; distribution unlimited.

13. SUPPLEMENTARY NOTES

The U.S. Government is joint author of this work and has the right to use, modify, reproduce, release, perform, display, or disclose the work. PA Case Number and clearance date: 88ABW-2011-6137, 28 Nov 2011. Preprint journal article to be submitted to Metallurgical Transactions. This document contains color.

14. ABSTRACT

While the role of borides on the microstructure of titanium alloys has been discussed in many previous reports, this paper presents the first experimental evidence of (a) the three-dimensional geometry of α precipitates confirming their equiaxed morphology, as determined by reconstruction of serially-sectioned scanning electron microscopy images and, (b) the influence of crystallographic orientation relationship between β, TiB, and α phases on the morphology of α precipitates, investigated via detailed orientation microscopy studies on a boron containing version of the commercial Ti-5Al-5Mo-5V-3Cr-0.5Fe (Ti5553) alloy.

15. SUBJECT TERMS

Ti5553, TiB, EBSD, crystallography, orientation relationship

16. SECURITY CLASSIFICATION OF:			17. LIMITATION OF ABSTRACT:	NUMBER OF PAGES	19a. NAME OF RESPONSIBLE PERSON (Monitor)
a. REPORT	b. ABSTRACT	c. THIS PAGE			Jay Tiley
Unclassified	Unclassified	Unclassified	SAR	16	19b. TELEPHONE NUMBER *(Include Area Code)* N/A

On the correlation between morphology of α and its crystallographic orientation relationship with TiB and β in boron containing Ti-5Al-5Mo-5V-3Cr-0.5Fe alloy

P. Nandwana[1], S. Nag[1], D. Hill[2], J. Tiley[3], H.L. Fraser[2], and R. Banerjee[1]

[1]Center for Advanced Research and Technology and Department of Materials Science and Engineering, University of North Texas, Denton, Texas, U.S.A.

[2]Center for the Accelerated Maturation of Materials and Department of Materials Science and Engineering, The Ohio State University, Columbus, Ohio, U.S.A.

[3]Air Force Research Laboratory, Wright Patterson Air Force Base, Dayton, Ohio, U.S.A.

Abstract

While the role of borides on the microstructure of titanium alloys has been discussed in many previous reports, this paper presents the first experimental evidence of (a) the three-dimensional geometry of α precipitates confirming their equiaxed morphology, as determined by reconstruction of serially-sectioned scanning electron microscopy images and, (b) the influence of crystallographic orientation relationship between β, TiB, and α phases on the morphology of α precipitates, investigated via detailed orientation microscopy studies on a boron containing version of the commercial Ti-5Al-5Mo-5V-3Cr-0.5Fe (Ti5553) alloy.

Keywords: Ti5553, TiB, EBSD, crystallography, orientation relationship.

Paper

There has been an increased interest in metastable β titanium alloys such as Beta21S (Ti-15Mo-2.6Nb-3Al-0.2Si, all compositions in wt.%) due to their attractive properties making them suitable candidates for applications requiring high specific strength and corrosion resistance. The excellent hot and cold

workability of these alloys give them an edge over conventional α+β alloys. However, rapid grain coarsening at elevated temperatures restrict the temperature range over which these alloys can be used [1]. It has been proved that Zener pinning by insoluble precipitates like TiB, by addition of trace amounts of boron during casting, is an effective way to minimize coarsening of prior β grains and has been extensively discussed in literature [2-6]. Apart from restricting grain growth at elevated temperatures, TiB precipitates have been reported to act as heterogeneous nucleation sites for α precipitation and have also been reported to alter the morphology of α by making it more equiaxed-like [3,7,8] as compared to the more classical lath-like morphology. Furthermore, the equiaxed α, in boron containing alloys, has been reported to exhibit multiple orientation relationships with the TiB precipitates. For example, while Hill et. al. [7] and Li et. al. [9] have reported an orientation relationship of $(0001)_{\alpha}$ // $(001)_{TiB}$ and $[11\bar{2}0]_{\alpha}$ // $[010]_{TiB}$, more recent studies by Sasaki et.al. [10] have shown the existence of multiple orientation relationships between α and TiB precipitates in the boron containing Beta21S alloy. However, the rationale behind the formation of equiaxed α and the role of orientation relationship between β and TiB in governing the morphology of α nucleating from TiB, has not been addressed in previously published literature. Therefore, the two primary aims of this paper are listed below:

(a) to determine the true three-dimensional morphology of α precipitates nucleating from boride precipitates present in the β matrix of a titanium alloy; and
(b) to investigate the role of presence or absence of orientation relationships between the α, β and TiB phases, on the morphology of α nucleating from TiB in the Ti5553 alloy..

The base Ti5553 and the boride reinforced Ti5553 alloys were processed by arc-melting in a conventional vacuum arc furnace. The boride reinforced Ti5553 composites were fabricated via an *in situ* reaction occurring during the arc-melting of pieces of commercial Ti-5Al-5Mo-5V-3Cr-0.5Fe (all in wt.%) alloy together with elemental boron powder. The base alloy will henceforth be referred to as Ti5553 and the

boron containing alloy as Ti5553-0.5B (due to the nominal addition of 0.5wt.%B). These alloys were subsequently sectioned into small pieces for heat treatment. Each sample was β-solutionized at 950°C for 30 minutes followed by furnace cooling to room temperature at an approximate cooling rate of 5°C/min. The samples were then mounted and polished using conventional metallographic techniques. The SEM and orientation microscopy (OM) studies were carried out using a FEI Nova 230 FEG NanoSEM equipped with an electron backscatter detector as well as an Electron Backscatter Diffraction (EBSD) detector. The OM studies allowed for the determination of orientation relationships between the β, TiB, and α phases present in the microstructure. Following the SEM studies, 3D microstructural information was acquired using a DualBeam™ focused ion beam instrument, the FEI DB235, which uses a gallium liquid metal ion source (LMIS) to mill the sample surface and serially section the microstructure. With each milling step, the microstructure was imaged with the electron beam and a custom-designed backscatter detector in the FIB. Subsequently the 3D microstructure was reconstructed using these backscatter SEM images.

Fig. 1(a) and (b) show representative backscatter SEM images of the microstructure of the base Ti5553 alloy and the Ti5553-0.5B alloy respectively, after β solutionizing and furnace cooling. Comparing these two images, the influence of the boride precipitate (exhibiting the darkest contrast in Fig. 1(b)) on the morphology of α precipitates is quite evident. While the classical lath-like morphology of the α precipitates that have either nucleated in an intra-granular fashion or from grain boundary α, is clearly visible in case of the base Ti5553 alloy (shown in Fig. 1(a)), the α precipitates associated with the boride precipitate exhibit a more equiaxed-like morphology in case of the Ti5553-0.5B alloy (shown in Fig. 1(b)). However, it is important to note that the three-dimensional (3D) morphology of these α precipitates cannot be uniquely determined based simply on these two-dimensional (2D) SEM images. Therefore, serial-sectioning of the Ti5553-0.5B alloy was carried out in a dual-beam FIB instrument and SEM

images were recorded after each stage of the serial-sectioning process. Fig. 1(c) shows one such 2D SEM image from this microstructure with the specific boride precipitate that was reconstructed marked within the box. Subsequently, this sequence of images were processed using standard image processing techniques and stacked up to reconstruct the true 3D morphology of both the boride precipitate as well as the α precipitates associated with the precipitate. An example of this is shown in the series of images (Figs. 1(d)-(f)), where different views of the 3D reconstructions of this boride precipitate and two α precipitates associated with this specific boride precipitate are shown. Viewing these α precipitates from different directions, their equiaxed morphology in 3D is clearly evident from this series of images. Additionally, it should be noted that the boride precipitate also exhibits a plate-like morphology in this 3D reconstruction.

The orientation relationships between the β, TiB, and α phases have been investigated in detail via OM studies carried out using an EBSD detector. Fig. 2(a) shows the overall phase map of one of the regions investigated in the Ti5553-0.5B sample. This map has been pseudo-colored with the yellow colored regions corresponding to the boride precipitates, the green colored regions corresponding to the β matrix phase, and the red colored regions corresponding to the α precipitates. The electron backscatter diffraction patterns as well as transmission electron diffraction patterns (not shown in the figure) from the boride precipitates could be consistently indexed based on the TiB phase with an orthorhombic B27 crystal structure. Three specific regions (1, 2 and 3) from this area of the microstructure have been marked in Fig. 2(a) and will be discussed subsequently. Fig. 2(b) shows a magnified view of Region 1, including three variants of α precipitates (α1, α2, and α3), none of which appear to be associated with any TiB precipitates. While Fig. 2(b) shows a pseudocolor map of the three α variants, the corresponding {0001}, $\{11\bar{2}0\}$, and $\{10\bar{1}0\}$ pole figures are plotted in Figs. 2(d), (e), and (f) respectively. Additionally, the {011}, {111}, and {112} pole figures for the matrix β grain, within which all three α variants appear

to have precipitated, are shown in Fig. 2(c). All the three α variants display a lath-like morphology and clearly exhibit Burgers Orientation Relationships (ORs) with the parent β matrix, given by $\{0001\}_\alpha$ // $\{011\}_\beta$ and $<11\bar{2}0>_\alpha$ // $<111>_\beta$ [11].

Fig. 3 shows a magnified pseudo-color map of Region 2 (from Fig. 2(a)) that includes a single TiB precipitate and three α precipitates (α_1, α_2, and α_3), belonging to different variants, that clearly appear to be associated with this boride precipitate. Furthermore, all three α precipitates shown in Fig. 3(a) exhibit near-equiaxed morphologies as compared to the lath-like α precipitates visible in Fig. 2(b). The relevant pole figures for the TiB precipitate and the three α precipitates are shown in Figs. 3(b), (c), (d) and (e) respectively. Additionally, the corresponding {011}, {111}, and {112} pole figures for the surrounding β matrix is shown in Fig. 3(f). From all these pole figure plots, it is noteworthy that the boride precipitate has distinct ORs with all three α precipitates. The OR between TiB and α_1 is $(0001)_\alpha$ // $(001)_{TiB}$ and $<11\bar{2}0>_\alpha$ // $[010]_{TiB}$ and henceforth will be referred to as OR1. Again, the OR between TiB and α_2 is $(0001)_\alpha$ // $\{101\}_{TiB}$ and $<11\bar{2}0>_\alpha$ // $[010]_{TiB}$ and will be referred to as OR2. Finally, the OR between TiB and α_3 is $\{01\bar{1}1\}_\alpha$// $(001)_{TiB}$ and $<11\bar{2}0>_\alpha$ // $[010]_{TiB}$ and will now be referred to as OR3. However, the interesting point to be noted is the absence of any OR between β and TiB as well as the fact that none of the three α precipitates exhibit the Burgers OR with the β matrix. Hence, the change in α morphology from lath-like (Fig. 2(b)) to near-equiaxed (Fig. 3(a)) can possibly be attributed to the loss of Burgers OR. Similar observations of the absence of a Burgers OR between near-equiaxed α precipitates and the surrounding β grain were made in several other regions of the same sample. Typically the Burgers OR between α precipitates and the surrounding β matrix, together with the anisotropy of their growth along different crystallographic directions, results in the development of their lath-like morphology [12]. The α/β interface has been reported to be semi-coherent along the broad face of lath-like precipitates. However, in the case discussed in Fig. 3, the lack of a specific Burgers OR is likely to result in an

incoherent α/β interface and would consequently lead to an more equiaxed-like morphology of the α precipitates.

Fig. 4(a) shows the magnified and pseudo-colored view of Region 3 in Fig. 2(a) where both the α precipitates (α_1, and α_2), display a lath-like morphology even though they appear to be nucleating from the TiB precipitate. It is evident from the pole figures, shown in Figs. 4(b), (c), (d), and (e), that TiB and α_1 showed the orientation relationship of OR3 while TiB and α_2 exhibited OR2. The fact to be noted, however, is that in this case the surrounding β grain displays an OR with TiB, $\{011\}_\beta$ // $(001)_{TiB}$ and $<111>_\beta$ // $[010]_{TiB}$. Therefore, the existence of orientation relationships between the β grain and the TiB precipitate, and between the TiB precipitate and α precipitates that appear to nucleate from it, permits the development of the Burgers OR between the β grain and both the α precipitates. Consequently these two α precipitates grow with a lath-like morphology, presumably with a semi-coherent α/β interface along the broad face of these laths. This contrast in α morphology compared to the previous case (Region 2) clearly indicates that the presence or absence of β/TiB OR plays a predominant role in determining whether Burgers OR between α and β would be present or not. This in turn governs the morphology of α precipitates that have nucleated from the TiB precipitates and are growing into the β matrix. It can also be said that the existence of an OR between β and TiB is primarily governed by whether or not the TiB precipitate nucleated adjacent to a β grain or directly within the boron-enriched liquid phase, in between the primary β grains, during hypoeutectic solidification.

The present study clearly elucidates the role of the crystallographic orientation relationships between the β, TiB, and α phases on the morphology of α precipitates in boron-containing titanium alloys. It provides first experimental evidence relating the dependence of morphology of α nucleating from TiB on the β/TiB OR. Also, the existence of multiple possible ORs between α precipitates and TiB has been clearly demonstrated, and in all cases it was observed that $<11\bar{2}0>_\alpha$ plane of the α phase was always parallel to the [010] plane of the TiB phase**.** A more detailed analysis of existence of multiple

orientation relationships between α and TiB is currently underway. Based on these results, it can be concluded that equiaxed α precipitates tend to heterogeneously nucleate from those TiB precipitates that do not exhibit a specific OR with the surrounding β grain. In contrast, those TiB precipitates that do exhibit an OR with the surrounding β grain, are more than likely to heterogeneously nucleate lath-like α precipitates, provided these α precipitates can maintain the Burgers OR with the β matrix.

References

[1] M. Peters, H. Buhl, in: H. Buhl (Ed.), Advanced Aerospace Materials, Springer-Verlag, Berlin, 1992, pp. 58-72.

[2] B. Cherukuri, R. Srinivasan, S. Tamirisakandala, D.B. Miracle; Scripta Materialia 60 (2009) 496-499.

[3] I. Sen, S. Tamirisakandala, D. B. Miracle, U. Ramamurty, Acta Materialia, 55 (2007) 4983-4993.

[4] S. Tamirisakandala, R.B. Bhat, J.S. Tiley, D.B. Miracle; Scripta Materialia 53 (2005) 421-426.

[5] S. Tamirisakandala, R.B. Bhat, J.S. Tiley, D.B. Miracle; Journal of Materials Engineering and Performance 14 (6) (2005) 741-426.

[6] S. Roy, S. Suwas, S. Tamirisakandala, D.B. Miracle, R. Srinivasan; Acta Materialia 59 (2011) 5494-5510.

[7] D. Hill, R. Banerjee, D. Huber, J. Tiley, H.L. Fraser; Scripta Materialia 52 (2005) 387-392.

[8] L. J. Huang, L. Geng, A. B. Li, F. Y. Yang, H. X. Peng, Scripta Materialia 60 (2009) 996-999.

[9] D.X. Li, D.H. Ping, Y.X. Lu, H.Q. Ye; Materials Letters 19 (1993) 322-326.

[10] T.T. Sasaki, B. Fu, K. Torres, G.B. Thompson, R. Srinivasan, B. Cherukuri, J. Tiley; Philosophical Magazine 91 (2011) 850-864.

[11] W.G. Burgers; Physica 1 (1934) 561-586.

[12] T. Furuhara, T. Makino, Y. Idei, H. Ishigaki, A. Takada, T. Maki; Materials Transactions, JIM, Vol. 39, No.1 (1998), 31-39.

Figure Captions

Fig1 Microstructures of (a) base Ti5553 alloy, (b)Ti5553-0.5B alloy, (c) TiB selected for serial sectioning and (d,e,f) TiB and associated α in three dimensional view.

Fig2 Represents (a) overall phase map with three distinct regions chosen for detailed study, (b) highlighted precipitates from Region1 and (c,d,e,f) corresponding pole figure maps.

Fig3 Represents (a) highlighted precipitates from Region2 of overall phase map and (b,c,d,e,f) corresponding pole figure maps.

Fig4 Represents (a) highlighted precipitates from Region3 of overall phase map and (b,c,d,e) corresponding pole figure maps.

Figures

Fig1

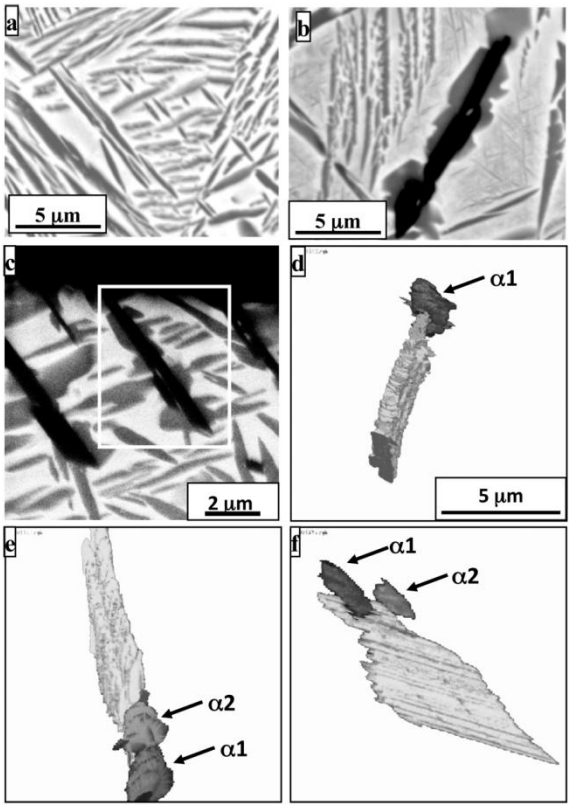

Fig2

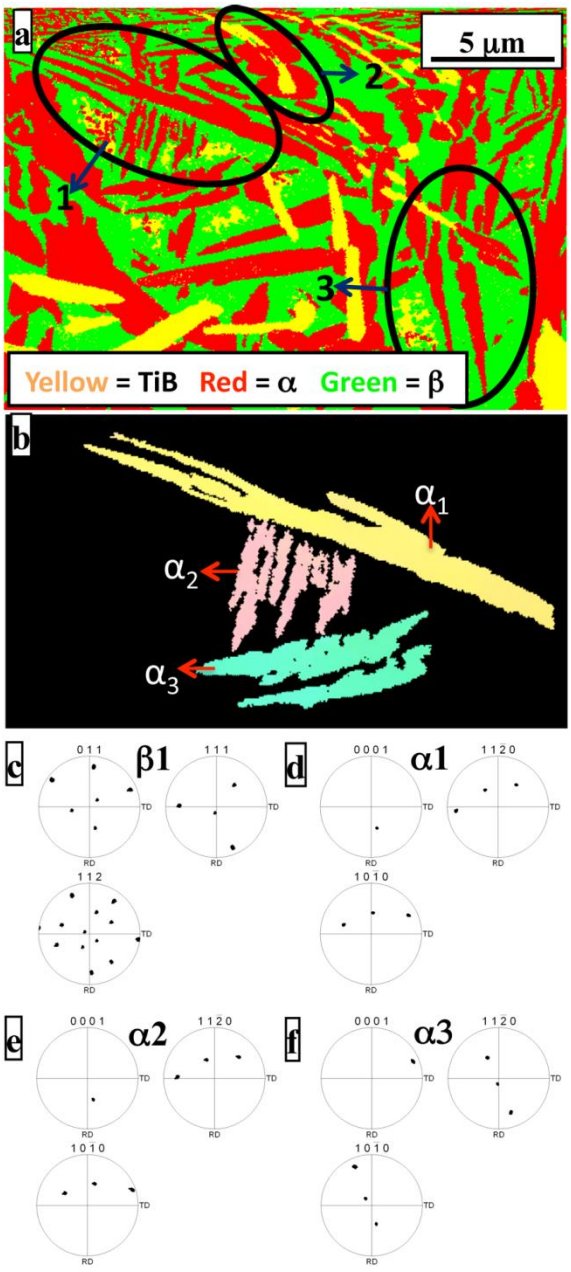

Fig3

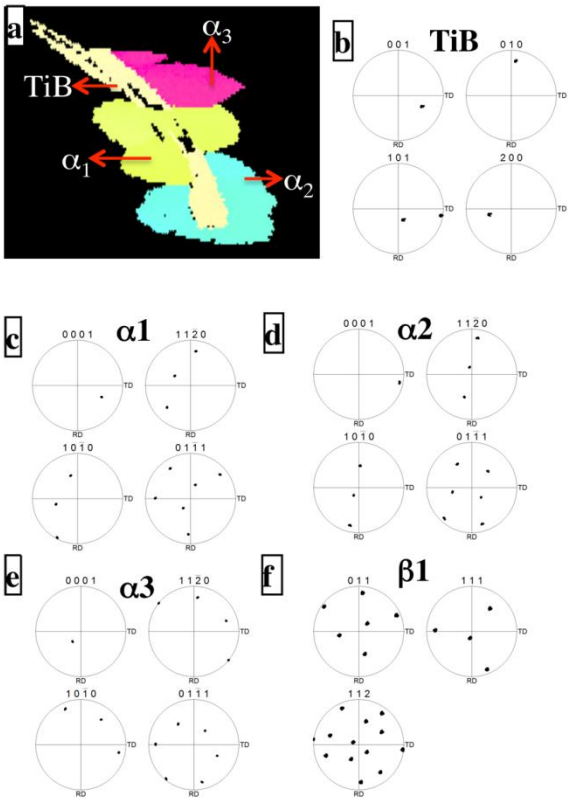

Fig4